JACS
JOURNAL OF THE AMERICAN CHEMICAL SOCIETY

ARTICLE

pubs.acs.org/JACS

The [NiFe]-Hydrogenase of the Cyanobacterium *Synechocystis* sp. PCC 6803 Works Bidirectionally with a Bias to H_2 Production

Chelsea L. McIntosh,[§] Frauke Germer,[‡] Rüdiger Schulz,[‡] Jens Appel,[†,‡] and Anne K. Jones*[,§,†]

[§]Department of Chemistry and Biochemistry and [†]Center for Bioenergy and Photosynthesis, Arizona State University, Tempe, Arizona 85287, United States

[‡]Botanisches Institut, Universität Kiel, Am Botanischen Garten 1-9, D-24118 Kiel, Germany

Supporting Information

ABSTRACT: Protein film electrochemistry (PFE) was utilized to characterize the catalytic activity and oxidative inactivation of a bidirectional [NiFe]-hydrogenase (HoxEFUYH) from the cyanobacterium *Synechocystis* sp. PCC 6803. PFE provides precise control of the redox potential of the adsorbed enzyme so that its activity can be monitored under changing experimental conditions as current. The properties of HoxEFUYH are different from those of both the standard uptake and the "oxygen-tolerant" [NiFe]-hydrogenases. First, HoxEFUYH is biased toward proton reduction as opposed to hydrogen oxidation. Second, despite being expressed under aerobic conditions *in vivo*, HoxEFUYH is clearly not oxygen-tolerant. Aerobic inactivation of catalytic hydrogen oxidation by HoxEFUYH is total and nearly instantaneous, producing two inactive states. However, unlike the Ni-A and Ni-B inactive states of standard [NiFe]-hydrogenases, both of these states are quickly (<90 s) reactivated by removal of oxygen and exposure to reducing conditions. Third, proton reduction continues at 25−50% of the maximal rate in the presence of 1% oxygen. Whereas most previously characterized [NiFe]-hydrogenases seem to be preferential hydrogen oxidizing catalysts, the cyanobacterial enzyme works effectively in both directions. This unusual catalytic bias as well as the ability to be quickly reactivated may be essential to fulfilling the physiological role in cyanobacteria, organisms expected to experience swings in cellular reduction potential as they switch between aerobic conditions in the light and dark anaerobic conditions. Our results suggest that the uptake [NiFe]-hydrogenases alone are not representative of the catalytic diversity of [NiFe]-hydrogenases, and the bidirectional heteromultimeric enzymes may serve as valuable models to understand the diverse mechanisms of tuning the reactivity of the hydrogen activating site.

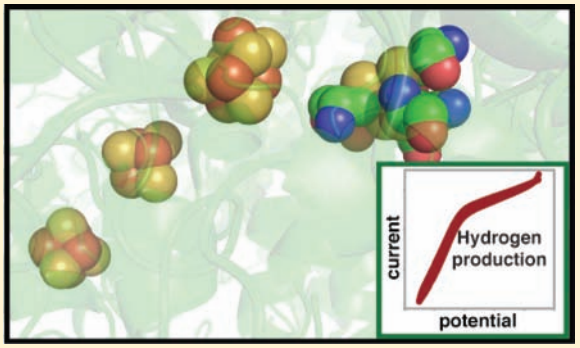

Hydrogen is an important currency in the energy economy of microorganisms, and many believe that biological systems may provide inspiration for overcoming some of the technological hurdles associated with a hydrogen fuel economy. Hydrogenases are the metalloenzymes that catalyze the reversible interconversion of protons and hydrogen; they are categorized according to active site metal composition as either [NiFe] or [FeFe].[1] Tantalizingly, like platinum metal, hydrogenases have been shown to catalyze both hydrogen oxidation and proton reduction with minimal electrochemical overpotential (driving force),[2,3] leading to their suggested use in a number of applications including photoelectrochemical devices and fuel cells.[3−6]

Since solar energy and water are two of our most abundant resources, coupling water splitting via oxygenic photosynthesis to fuel production via hydrogenases is a particularly attractive pathway.[7−11] Cyanobacteria and green algae are, at present, the only known organisms that both produce hydrogenases and are capable of performing oxygenic photosynthesis.[12−16] Utilizing green microalgae such as *Chlamydomonas reinhardtii*, methods for direct, sustained photoproduction of hydrogen have been established.[17] This is, however, technically challenging, as algae produce [FeFe]-hydrogenases, enzymes noted for their fast hydrogen production but also for extreme and irreversible sensitivity to oxygen.[18−22] In addition to the oxygen sensitivity of the enzymes themselves, both hydrogenase gene expression and biosynthesis appear also to be oxygen-sensitive in green algae.[15,23,24]

Cyanobacteria, on the other hand, utilize [NiFe]-hydrogenases in their hydrogen metabolism. Despite being considered generally less efficient for hydrogen production than the [FeFe]-hydrogenases, [NiFe]-hydrogenases may be more useful for technological applications as they are only reversibly inhibited by molecular oxygen, and some, produced in aerotolerant organisms, are able to function in the presence of oxygen, a property no characterized [FeFe]-hydrogenase has exhibited.[25−32] Substantial effort has gone into understanding the mechanisms of inactivation of [NiFe]-hydrogenases as well as identifying means by which more aerotolerant enzymes may be developed.[33] Model [NiFe]-hydrogenases from several organisms including *Allochromatium vinosum*,[34−37] *Aquifex aeolicus*,[32] *Desulfomicrobium baculatum*,[38]

Received: April 12, 2011
Published: June 15, 2011

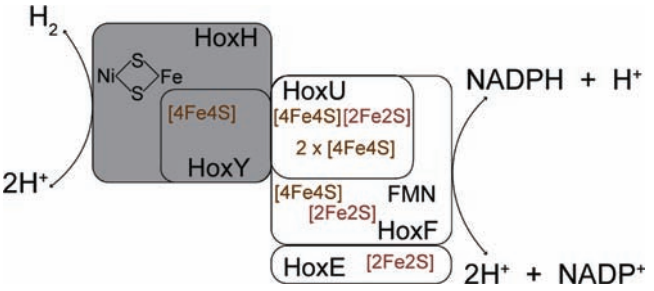

Figure 1. Cartoon of the subunit composition of the heteropentameric HoxEFUYH and the hypothetical cofactors contained in each protein component.

Desulfovibrio fructosovorans,[28,39] *Escherichia coli*,[30] and *Ralstonia eutropha*[26,27,29,40] have been catalytically characterized *in vitro*. Although [NiFe]-hydrogenases are widely distributed throughout archaea and bacteria, notably missing from this list of organisms are cyanobacteria. Additionally, despite the fact that [NiFe]-hydrogenases have been phylogenetically divided into four distinct groups,[41] all of the established model systems are representatives of the "uptake", also known as group 1, class, a group of heterodimeric, monofunctional enzymes thought to catalyze hydrogen oxidation *in vivo*. However, two functionally distinct [NiFe]-hydrogenases are present in the cyanobacteria, an uptake and a bidirectional enzyme, and the latter is thought to interact with photosynthetic pathways.[42−44] Enzymes of the cytoplasmic, bidirectional group of [NiFe]-hydrogenases have been much less studied than those from the uptake group. They are heteromultimeric, bifunctional enzymes usually coupling proton/hydrogen interconversion at the [NiFe] active site with NAD(P) reduction at a flavin mononucleotide active site.

Synechocystis sp. PCC 6803 is a non-nitrogen fixing cyanobacterium and thus produces only a bidirectional enzyme of the NAD(P)-reducing class.[45] The precise physiological role of this enzyme is still under debate, but it is believed to function as an electron valve for an excess of electrons produced under photosynthetic and fermentative conditions.[46−49] The heteropentameric enzyme, HoxEFUYH (Figure 1), in which HoxY and HoxH form the hydrogenase and HoxE, HoxF and HoxU the diaphorase subunit, is highly homologous to both the soluble [NiFe]-hydrogenase from the knallgas bacterium *Ralstonia eutropha* and part of the peripheral subunits of respiratory Complex I.[45,50−55] Although [NiFe]-hydrogenases are usually described as functioning primarily in the hydrogen oxidation direction, HoxEFUYH is involved in fermentative hydrogen production as well as working as an electron valve when photosynthesis resumes under anaerobic conditions.[46−49,56] The possibility for this enzyme to catalyze hydrogen production efficiently and with limited sensitivity to oxygen has caused HoxEFUYH to be identified as a candidate for use in technologies.

HoxEFUYH from *Synechocystis* sp. PCC 6803 has recently been homologously overexpressed, purified and spectroscopically characterized via EPR and FTIR revealing for the first time that the active site of a [NiFe]-hydrogenase from an oxygenic phototroph also contains the now standard two cyanides and a single carbon monoxide observed in all other [NiFe]-hydrogenases characterized.[57] However, despite the seemingly orthodox nature of the active site, several significant spectroscopic differences from the so-called standard (uptake) hydrogenases were observed. First, paramagnetic Ni states were not observed in samples of any redox state of HoxEFUYH, a property shared with other bidirectional [NiFe]-hydrogenases such as those from *Anabaena variabilis*,[58] *Pyrococcus furiosus*,[59] *Nocardia opaca* 1b,[60] and *Allochromatium vinosum*.[61] This is remarkable since the standard, uptake enzymes can be isolated in three distinct paramagnetic Ni states: Ni-A, Ni-B and Ni-C, and suggests that in HoxEFUYH either the Ni remains in a diamagnetic state [Ni(II)] throughout the catalytic cycle or is coupled to a nearby paramagnet resulting in an overall diamagnetic state (see Scheme 1 for a summary of the known spectroscopic states of [NiFe]-hydrogenases). Of the EPR-active Ni states identified for uptake hydrogenases, Ni-A and Ni-B are both catalytically inactive, and the suggestion that the *Synechocystis* HoxEFUYH may have decreased susceptibility to oxidative inactivation is appealing. Second, of the eight major states of standard, uptake [NiFe]-hydrogenases detected via FTIR spectroscopy, only four analogous states were identified in studies of the *Synechocystis* HoxEFUYH. In particular, states assigned as Ni-B-like, Ni-SI_a-like, Ni-C, and Ni-R were observed via FTIR. We note for clarity that the Ni-B-like state observed for HoxEFUYH via FTIR spectroscopy did not have a corresponding Ni EPR signal. Consistent with the EPR results, the catalytically inactive states, Ni-A, Ni-SU, and Ni-SI_r, were not detected via FTIR. Similar FTIR results for the highly homologous cytoplasmic soluble bidirectional enzyme from *Ralstonia eutropha* have recently been reported using *in situ* spectroscopy of whole cells suggesting that the spectroscopically observed states are perhaps also the physiologically relevant ones.[55,62] Third, many of the eight [2Fe2S] or [4Fe4S] clusters thought to be present in HoxEFUYH based on highly conserved [FeS] cluster binding motifs,[51,57,60] could not be observed via EPR spectroscopy. Only one [4Fe4S] and at least one [2Fe2S] cluster, both magnetically coupled to one another, were detected. A small signal from a $[3Fe4S]^+$ cluster quantitated at a mere 0.05 spins/protein is believed to be the result of oxidative damage of a [4Fe4S] cluster. This is remarkable since all known uptake hydrogenases harbor a [3Fe4S] cluster, the reduction potential of which is much higher than the other redox cofactors in the enzyme.[63] The structural basis or functional consequences of these spectroscopic differences from standard uptake hydrogenases are not yet clear.

Protein film electrochemistry (PFE) is a technique in which a redox enzyme is adsorbed onto an electrode surface in a configuration allowing direct electron transfer without chemical mediators, and activity is simply monitored as current.[64,65] The precise ability to control electrode and hence enzyme potential afforded by PFE has been used to great effect for studying both catalytic activity and potential in/activation of [NiFe]- and [FeFe]- hydrogenases over the past decade.[2,4,18,19,22,30−32,34−39,64−66] Furthermore, since the enzyme is adsorbed to the electrode tip, transfer of the enzyme-covered electrode between solutions of various compositions can be used to quickly characterize the *in vitro* catalytic activity under a wide range of precisely defined experimental conditions.

In this paper, we report the first PFE characterization of either a multimeric bidirectional [NiFe]-hydrogenase or a cyanobacterial [NiFe]-hydrogenase. We describe the activity toward both proton reduction and hydrogen oxidation as well as the unusual (in)activation under anaerobic and aerobic conditions. The results are compared to standard uptake and oxygen-tolerant uptake [NiFe]-hydrogenases, and HoxEFUYH is shown to have unique reactivity. Structural explanations for this unique functionality will be considered.

■ MATERIALS AND METHODS

The purification of the enzyme was reported in ref 57. Protein film electrochemistry experiments were carried out in a glovebox filled with

Scheme 1. Schematic Overview of the Spectroscopically Identified Redox Intermediates in Standard, Oxygen-sensitive [NiFe]-Hydrogenases (Left), HoxEFUYH from *Synechocystis* sp. PCC 6803 (Middle), and O_2-Tolerant Uptake [NiFe]-Hydrogenases[a]

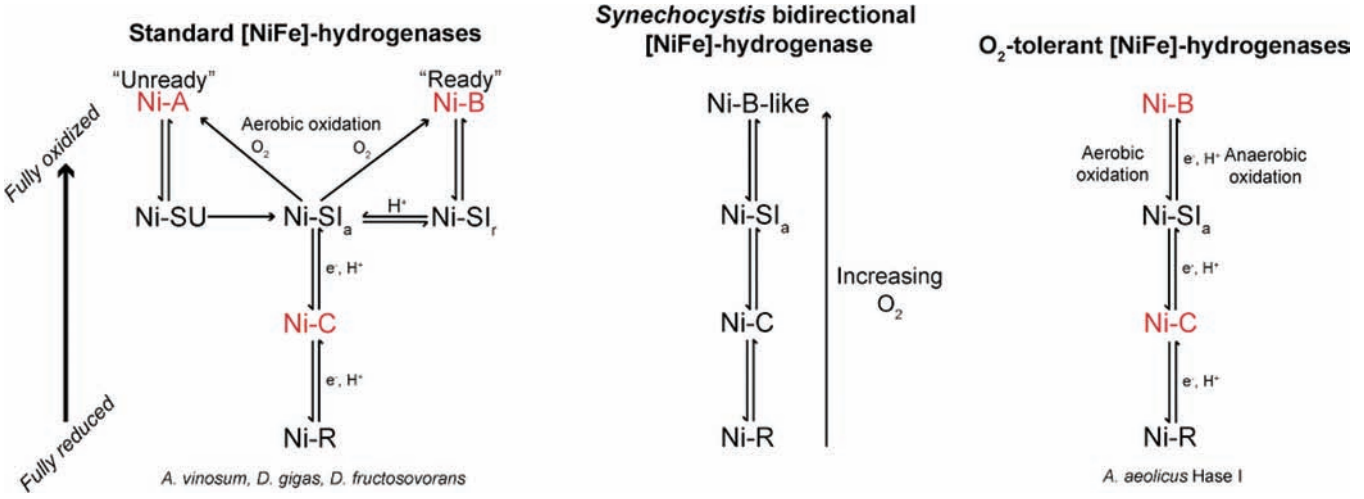

[a] EPR active states are denoted in red and the EPR-silent states in black. The most oxidized states appear at the top of the diagram and the most reduced at the bottom. States believed to be analogous and/or at the same redox level are horizontally aligned across the figure.

nitrogen (Vacuum Atmospheres, O_2 < 4 ppm) in a glass cell with a machined Teflon cap designed to stabilize electrode placement. The potentiostat was a PG-STAT 128N Autolab electrochemical analyzer (Eco Chemie, Utrecht, The Netherlands) controlled by GPES software. A saturated Ag/AgCl electrode was used as reference and a platinum wire as counter electrode. All potentials were corrected to the standard hydrogen electrode (SHE) according to the equation $E_{SHE} = E_{Ag/AgCl} +$ 197 mV at 25 °C.[67] Pyrolytic graphite "edge" (PGE) working electrodes were constructed by attaching a cylindrical piece of graphite (r = 2.5 mm, Minteq) to a steel rod via a silver-loaded epoxy (AI Technologies, Princeton Junction, NJ) that was then inserted into a Teflon sheath. The exposed graphite was then encased within an adhesive epoxy (Epoxies Etc., Cranston, RI). The rotating working electrode was used in conjunction with an AFMSRCE Series Rotator (Pine Instrument Co.).

All chemicals were of the highest grade commercially available and were used without further purification. Solutions for electrochemical experiments were prepared using purified water (resistivity 18.2 MΩ cm^{-1}). The mixed buffer consisted of 15 mM each of 4-(2-hydroxyethyl)-1-piperazineethanesulfonic acid (HEPES), 2-[N'-cyclohexyl-amino]ethanesulfonic acid (CHES), 2-[N'-morpholino]ethanesulfonic acid (MES), N'-tris[hydroxymethyl]methyl-3-amino-propanesulfonic acid (TAPS), and sodium acetate with 0.1 M NaCl as supporting electrolyte (HEPES, CHES, TAPS, and sodium acetate from Sigma, MES from USB Corporation, NaCl from VWR). Solutions were adjusted to the desired experimental pH with either NaOH or HCl. The experimental pH and temperature for each experiment are indicated in the figure legend. Gas mixtures were purchased from Air Liquide American and used as received.

Enzyme films were prepared by first polishing the electrode with a 1 μm aqueous alumina (Buehler) slurry followed by thorough sonication and rinsing. The electrode was then inserted into a cell containing dilute (0.1−1 μM) enzyme solution and cycled between the potentials +197 and −603 mV at a scan rate of 10 mV/s until the reductive catalytic current stabilized. The enzyme solution was then removed from the cell and replaced with pH 6.4 buffer solution. The electrode potential was again cycled until current stabilized.

The electrochemical data were analyzed with SOAS, an electrochemical program freely available for download on the Internet at http://bip.cnrs-mrs.fr/bip06/software.html.[68]

RESULTS

1. Catalytic Activity and Bias. As shown in Figure 2A, HoxEFUYH adsorbs to a PGE electrode and catalyzes the electrolytic reduction of H^+ under a N_2 atmosphere; the magnitude of the catalytic current is directly proportional to the activity of the enzyme on the electrode surface. Electrode rotation can be used to control flux of substrate to the electrode surface. At low electrode rotation rates, the catalytic current depends on rotation rate, indicating that it is limited by mass transport of substrate to the electrode surface or diffusion of inhibitor away from the surface. However, at moderate rotation rates, 1000 rpm or greater, the observed voltammetry is unaffected by increasing rotation rate. Thus all experiments have been undertaken at 1000 rpm or greater. Absolute current magnitude depends also on the quantity of enzyme on the electrode surface,[69] and, although catalytic activity is clearly observed for this enzyme, noncatalytic signals have not been observable, making quantification of the amount of enzyme on the electrode surface impossible. Thus, in order to compare activities from experiments with different protein films and, correspondingly, different quantities of active enzyme on the electrode surface, data have been normalized to a standard condition: pH 6.4. At this intermediate pH value, the film is relatively stable and, as demonstrated below, displays considerable activity for both proton reduction and hydrogen oxidation. In short, the activity was first measured in a reference buffer of pH 6.4. Then the experiment of interest was performed, and finally the activity was again measured in a buffer of pH 6.4 to monitor any change in electroactive coverage. Data are presented normalized so that the activity at pH 6.4, averaged before and after the experiment, is 1.

The catalytic reduction of H^+ by HoxEFUYH at −560 mV increases with decreasing pH (Figure 2B). This may be an effect of either the substrate (proton) concentration or the protonation state of the enzyme as a whole. Additionally, there may be a pH optimum in the region of 5.5, but instability of the enzyme on the electrode surface at low pH values precludes reaching any definitive conclusion.

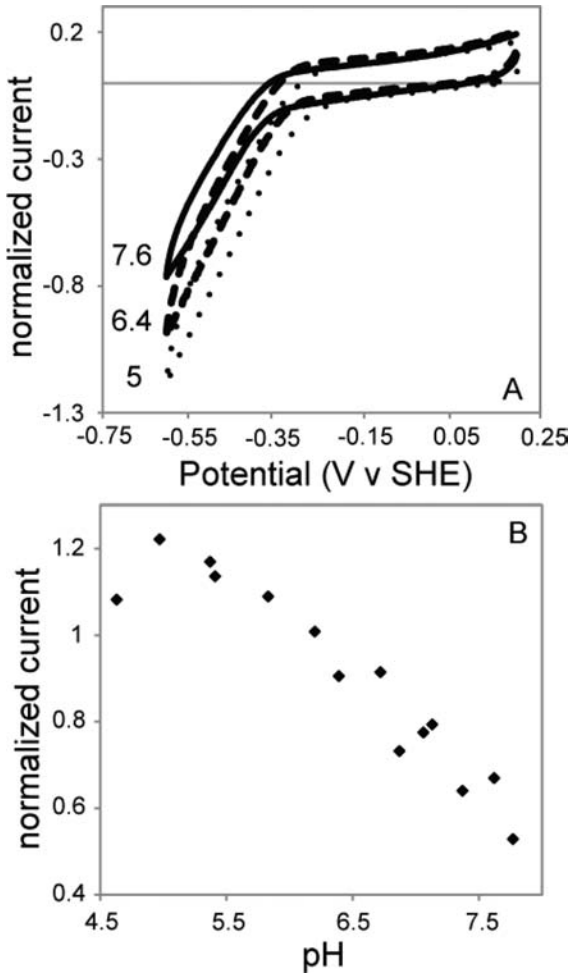

Figure 2. (A) Proton reduction catalytic voltammograms for HoxEFUYH at various pH values normalized as described in the text. Experiments were performed at 25 °C with an electrode rotation rate of 1000 rpm in a 75 mM mixed buffer consisting of 15 mM each of HEPES, CHES, MES, TAPS and sodium acetate adjusted with NaOH or HCl to reach the desired pH value. Additionally, 0.1 M NaCl was added as supporting electrolyte. Scans were initiated from the oxidative potential limit at a rate of 10 mV/s. (B) Normalized reduction activity at −560 mV derived from voltammograms such as those shown in panel A.

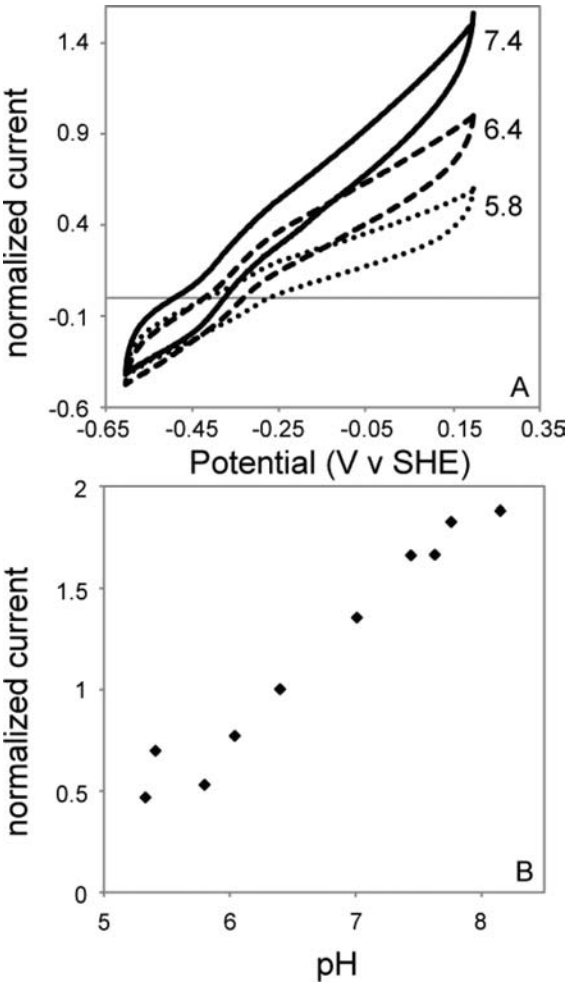

Figure 3. (A) Catalytic voltammograms of adsorbed HoxEFUYH in the presence of 1 atm hydrogen at various pH values. Experimental conditions are as in Figure 2 except that 100% hydrogen is equilibrated into the solution, and the electrode is stationary. H_2 was equilibrated into each solution by flowing a gas stream over the top for five minutes before the scan and continuing to flow during scanning. (B) Normalized H_2 oxidation activity at +197 mV as a function of pH.

With respect to the shape of the voltammograms, there are two features worth noting. First, the onset of reductive catalysis, the potential at which the catalytic voltammograms begin to deviate from a blank electrode, mirrors the potential of the standard hydrogen couple, i.e., no noticeable electrochemical overpotential is required to induce catalysis. Second, as seen for many other hydrogenases, the shape of the voltammograms is not sigmoidal as might be predicted from simple models but instead nearly linear and does not reach a sharp plateau at high driving forces (i.e., very low potentials). This phenomenon can be explained, as first demonstrated by Léger and co-workers, by assuming that the enzyme molecules are adsorbed to the electrode in a distribution of states and that the interfacial electron transfer rate depends on enzyme orientation.[70] The extreme linearity of these voltammograms thus suggests that the rate of reductive electrocatalysis is significantly influenced by slow interfacial exchange of electrons between the enzyme and electrode.

Voltammograms recorded in the presence of hydrogen report on the ability of the enzyme to oxidize hydrogen. As shown in Figure 3, HoxEFUYH adsorbed to PGE is also catalytically competent in the hydrogen oxidation reaction on an electrode surface. Several differences were observed relative to the voltammetry in a nitrogen atmosphere. First, in the presence of hydrogen, proton reduction activity is significantly decreased but not completely eliminated. As for many other hydrogenases studied to date, this demonstrates that the proton reduction catalysis is severely product inhibited by hydrogen.[35] Second, the voltammetry does not have any noticeable rotation rate dependence (data not shown) indicating that hydrogen oxidation is not limited by transport of hydrogen to the electrode surface. This most likely indicates that the electroactive coverage of the enzyme on the electrode surface is relatively sparse. With respect to coverage, it is worth noting that as opposed to the heterodimeric uptake [NiFe]-hydrogenases, the pentameric HoxEFUYH is a substantially heavier enzyme. Thus we may expect the maximum coverage on the electrode surface to be lower than for other hydrogenases studied via PFE to date. As was the case

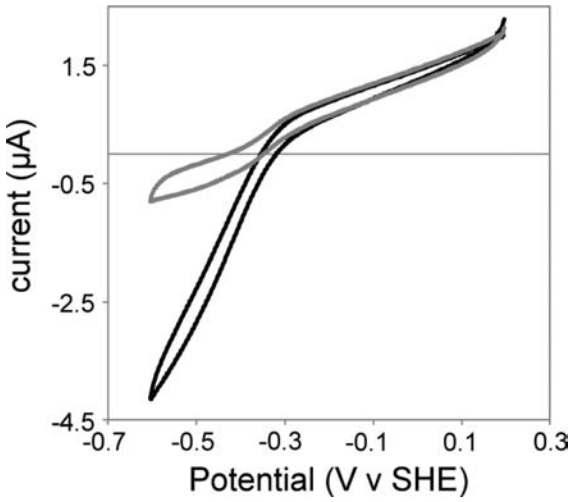

Figure 4. Comparison of the electrocatalytic currents obtained for hydrogen oxidation and proton reduction by HoxEFUYH from *Synechocystis*. The black voltammogram was recorded first in an atmosphere of trace hydrogen in nitrogen followed by the gray voltammogram under 1 atm H_2. Experimental conditions are as described in Figure 2, and the experimental pH is 6.4. The electrode is rotated at 1000 rpm.

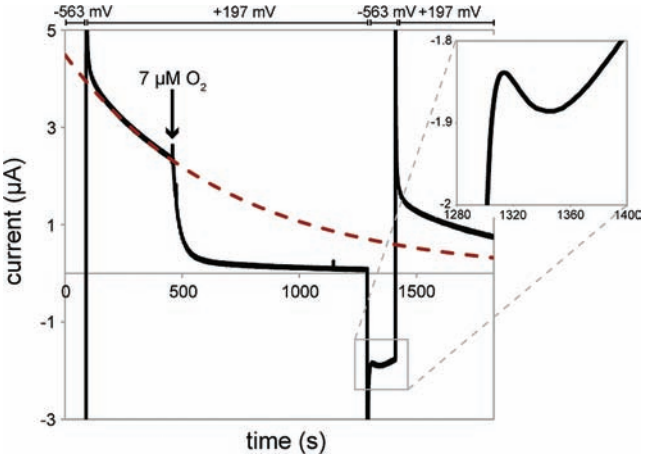

Figure 5. Potential step experiment showing the effect of O_2 on H_2 oxidation activity and time scale of enzymatic recovery after a jump to negative potentials. The electrode was first held at −563 mV for 90 s to ensure full activation of enzyme film. After 90 s, the potential was jumped to +197 mV for 1200 s. At ∼500 s, 7 μM O_2 is injected into the cell. The O_2 injected is removed from the cell by a constant stream of 5% H_2 in N_2. At time 1290 s, the electrode is stepped back down to −563 mV for 120 s to reactivate the inactive enzyme. After reactivation, the electrode is then stepped back up to +197 mV to monitor the extent of reactivation. The black line is experimental data, the red dashed line is a single exponential fit to the oxidative activity before oxygen injection to account for film loss. Other experimental conditions: mixed buffer pH 6.4 under 5% H_2 in N_2, T = 25 °C, electrode rotation rate of 1500 rpm.

for the reductive catalytic experiments, to facilitate comparison between different experiments, voltammograms have been normalized relative to signals in pH 6.4 buffer. Figure 3B clearly shows that the rate of oxidation of hydrogen at +197 mV by HoxEFUYH increases, tripling between pH 6 and pH 8, as the solution pH increases. This marked pH dependence is quite different from what was observed for both *Allochromatium vinosum* and *Desulfovibrio fructosovorans* both of which have pH independent hydrogen oxidation activity.[35,39]

[NiFe]-hydrogenases are often described as biased in the direction of hydrogen uptake. However, the data in Figures 2−4 demonstrate that this is not the case for HoxEFUYH. Figure 4 shows voltammograms, and thus maximal catalytic currents, arising from a single HoxEFUYH enzyme film both in the presence and absence of hydrogen at pH 6.4. Thus we can directly compare the activities in the proton reduction and hydrogen oxidation directions under these conditions. At high driving forces, in the absence of hydrogen, 4.1 μA of proton reduction catalytic current was observed. Similarly, at high overpotentials in hydrogen saturated solution, 2.1 μA of hydrogen oxidation catalytic current was observed. Since current is directly proportional to catalytic activity, Figure 4 demonstrates that at pH 6.4 the proton reduction rate by HoxEFUYH (for a solution saturated with nitrogen) is approximately 2 times faster than hydrogen oxidation (for a solution saturated with hydrogen).

It is interesting also to compare proton reduction to hydrogen oxidation activities at other pH values. Since the amount of electroactive enzyme on the electrode is not quantifiable and may vary for each film prepared, this comparison must been made through a single enzyme film. This is made possible by comparing the normalized experiments in Figures 2 and 3 to the absolute data provided in Figure 4. For example, Figure 2 shows that the optimum of activity for hydrogen oxidation occurs at high pH and corresponds to an activity approximately 1.6 times that at pH 6.4. We can think of this as 3.4 μA if measured for the same film used in Figure 4. On the other hand, as shown in Figure 3, the optimum for proton reduction occurs at low pH, and the activity is 1.2 times that at pH 6.4, i.e., 4.9 μA if measured for the same film used in Figure 4. Using these absolute currents, in a sense extrapolated from the pH 6.4 values, we conclude that proton reduction activity at low pH is about 1.4 times faster than hydrogen oxidation activity at high pH. Therefore, HoxEFUYH can be described as moderately biased in the direction of hydrogen production. Extrapolated current values for all pH values measured are summarized in the Supporting Information, Table S1. This allows direct comparison of activities at any desired combination of pH values. Excluding [NiFeSe]-hydrogenases, [NiFe]-hydrogenases are usually thought of as significantly biased toward hydrogen oxidation. The only exception in the literature is Hyd-2 from *Escherichia coli*, an enzyme that has been demonstrated to be bidirectional, i.e., hydrogen oxidation activity is only two times as fast as proton reduction activity at pH 6 (see Figure 1 in ref 30). HoxEFUYH, with its moderate bias toward proton reduction, thus shifts the balance of catalytic activities farther than any other [NiFe]-hydrogenase characterized to date.

2. Reactions of HoxEFUYH with O_2. Figure 5 demonstrates via chronoamperometry the reaction of HoxEFUYH with oxygen under oxidizing conditions. Unlike the so-called oxygen-tolerant [NiFe]-hydrogenases, HoxEFUYH does not oxidize hydrogen in the presence of oxygen; however, HoxEFUYH quickly recovers when oxygen is removed from the system and reducing conditions are briefly restored. Initially, the enzyme-covered electrode was held at an oxidizing potential in an atmosphere of 5% hydrogen to observe catalysis and establish a baseline for decay of film activity. The slow decay of the activity (considered below) could be fit to a single exponential curve shown by the red dashed line. At time 500 s, an aliquot of air-saturated buffer was injected into the system for an initial oxygen concentration of 7 μM and

an immediate drop of the catalytic current to zero was observed, indicating inactivation of the enzyme. The oxygen was then removed from the system by a constant stream of 5% hydrogen in nitrogen (control experiments in Supporting Information demonstrate that 700 s was sufficient to remove all of the oxygen from the system, Figure S1). However, unlike the so-called "oxygen-tolerant enzymes", the activity of the enzyme was not recovered simply by removal of oxygen. Instead, it was absolutely necessary to decrease the potential of the system to reductively reactivate the enzyme and regain catalytic activity. As shown in the inset of Figure 5, an increase in catalytic proton reduction current (more negative current) was observed as soon as the enzyme was reactivated. This trace suggests that reactivation of the oxygen inactivated state was complete at −563 mV within 60−90 s. After reactivation, the electrode was biased again to an oxidizing potential (+197 mV) to observe the recovery of the hydrogen oxidation catalysis. Analogous control experiments in which no oxygen was introduced into the system did not undergo any observable reductive reactivation (Figure S2) indicating that the inactive species requires oxygen for formation.

As shown in Figure 5, surprisingly, the oxidation activity observed after reactivation was more than would have been expected if oxygen had not been introduced into the cell (the activity predicted by the red dashed line). In order to explain this phenomenon, a control chronoamperometry experiment in which nitrogen saturated (as opposed to air saturated) buffer was injected into the cell and the electrode was then disconnected from the potentiostat was performed (Figure S3). This experiment demonstrated that no decay of activity occurred while the enzyme coated electrode was disconnected from the electrochemical cell, i.e., the activity remained at precisely that observed immediately prior to disconnection. This result suggests that the enzyme is not inherently unstable on the electrode surface, an observation confirmed by long-term (days or weeks) stability of unused enzyme coated electrodes stored in the glovebox (data not shown). Instead, catalytic turnover itself appears to cause the irreversible loss of catalytic activity. Thus, the red curve in Figure 5 is not the most relevant predictor of catalytic activity after the introduction of oxygen and reactivation. Instead, it may be expected that the maximum activity that could be attained after reactivation is the activity observed immediately before injection of oxygen, since film loss should be minimal, i.e., drops effectively to zero, while the enzyme is (aerobically) oxidatively inactivated and not turning over. As described below, the extent of reactivation can be monitored as a function of reductive potential, and indeed, the current observed immediately before introduction of oxygen serves as a limit to the activity that can be observed after reactivation.

To investigate the thermodynamics of reactivation of the inactive state produced after O_2 injection, the experiment depicted in Figure 5 was repeated varying only the reduction potential of the reactivation step. The extent of reactivation was then quantified as the ratio of the oxidation current from the second oxidizing jump to the oxidation current obtained immediately before the injection of O_2. The results are compiled in Figure 6. The data in this figure were normalized so that the fraction obtained at the most negative reactivation potential is 1, i.e., full reactivation. The resulting data were fit with the Nernst equation,

$$\text{fraction reactivated} = \frac{1}{1 + exp\left(\frac{nF}{RT}(E - E_{mid})\right)} \quad (1)$$

where F is Faraday's constant, R is the gas constant, T is the temperature, n is the number of electrons, and E_{mid} is the midpoint potential of reactivation of the inactive state. The model best matches the data when $n = 1$ and $E_{mid} = -372$ mV, shown as the red line in Figure 6. It should be noted here that even at the most oxidizing reactivation potentials (specifically −200 to −100 mV) some activity was always recovered. This suggests that a second, minor species is formed during inactivation that reactivates at a higher potential, and we return to this topic below.

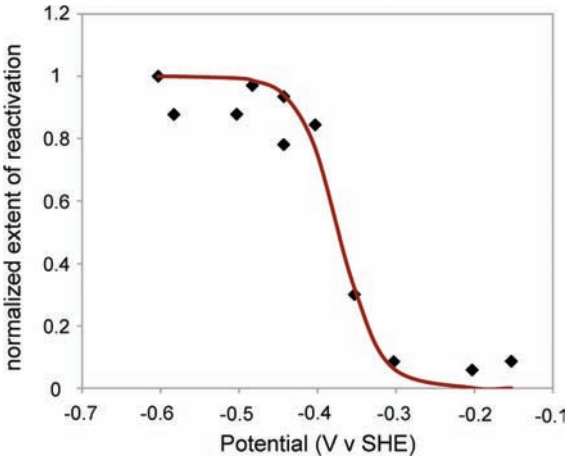

Figure 6. Fraction of enzyme reductively reactivated after O_2 inhibition as a function of potential. Values have been normalized assuming that the reactivation at −600 mV is 1 (i.e., complete reactivation after allowing for film degradation). The black diamonds are experimental data. The solid red line is a fit to a Nernstian equation. The experimental conditions for all data collected were: T = 25 °C, pH 6.4, electrode rotating at 1500 rpm under 5% H_2 in N_2. The chronoamperometric experiments used to generate the data included the following series of potential steps: (1) −563 mV for 90 s to ensure complete activation of the enzyme, (2) +197 mV for 1200 s to observe oxidation activity, establish background for film desorption/denaturation and introduce oxygen; 1200 s is long enough to ensure that oxygen is effectively removed from the cell before returning to reductive potentials, (3) 120 s reductive pulse at variable potentials to reactivate inactive enzyme, (4) +197 mV for 420 s to quantify the extent of enzyme reactivation. For each experiment, air-saturated buffer was injected into the cell (0.25 mL into 4.75 mL, V_{final} = 5 mL) at ∼450 s, for a total initial concentration of 14 μM O_2.

3. Detection of a Second Oxidized Inactive Species. As described above, chronoamperometric experiments to characterize the oxygen inactivated state of HoxEFUYH provided hints that not one but two distinct oxidized, inactive states may be formed since a small population of the enzyme was always reactivated at higher potentials. Although only one oxidized, inactive state of HoxEFUYH, labeled the "Ni-B-like" state, has been detected via FTIR spectroscopy,[57] standard, uptake [NiFe]-hydrogenases have been shown to produce two species distinguished primarily by their rate of reactivation (see Scheme 1). These EPR-active but catalytically inactive states are usually referred to as Ni-B (or Ni-ready) and Ni-A (or Ni-unready).[71] The Ni-B state can be reduced to a catalytically active form within seconds whereas the Ni-A state requires reduction for longer time periods (tens of minutes) to regain activity. Only the Ni-B state is formed during anaerobic, oxidative inactivation, but a mixture of Ni-A and Ni-B states forms under aerobic conditions depending on electrochemical potential as well as hydrogen and oxygen concentration.[37] By way of comparison, it is important to recall that no EPR signals from Ni have been detected in any of the redox states of HoxEFUYH.

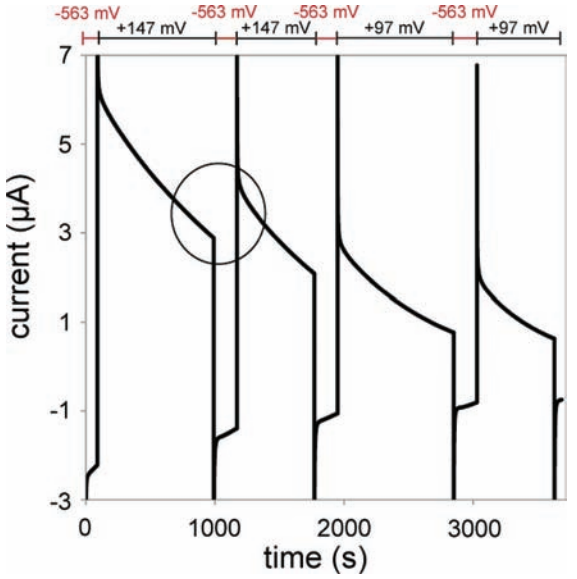

Figure 7. Chronoamperometry experiments probing anaerobic oxidative inactivation. The location and duration of the reducing potential (−563 mV) is indicated in red above the scan, whereas the various oxidative potentials are indicated in black. The enzyme was first held at −563 mV for 90 s to ensure fully active enzyme. The potential was then stepped to the oxidative values for intervals indicated in the figure. The duration of the step down to reducing potentials (−563 mV) following each oxidative pulse to reactivate the enzyme was 180 s. The circle indicates the region in which recovery of oxidative activity can be observed for the first reactivation. Other experimental conditions: pH 7.5 buffer, 5% H_2 in N_2, T = 25 °C, electrode rotation rate 1500 rpm.

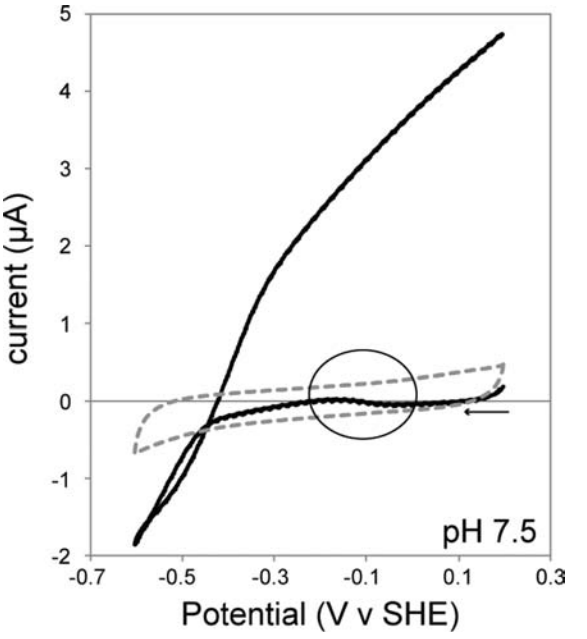

Figure 8. Detection of a second, higher potential reactivating, catalytically inactive, oxidized species via cyclic voltammetry after O_2 injection. Experiment was conducted under the following conditions: A HoxEFUYH coated electrode was placed in an electrochemical cell containing pH 7.5 buffer under a 5% H_2 atmosphere rotating at 1500 rpm. The first scan, where 14 μM O_2 is injected at −200 mV to inactivate the enzyme, is not shown. After inactivating the enzyme and exchanging the cell solution to buffer of the same compistion with *no* O_2, the scan was reinitiated at +197 mV (black trace above). The circle illustrates partial regain in oxidative activity at ∼−100 mV, whereas the remaining enzyme does not reactivate until potentials more reductive than the H_2 couple. The scan then returns to +197 mV with active enzyme, as indicated by the large H_2 oxidation current seen. The gray dashed line is a blank of the electrode without enzyme to illustrate the baseline current.

With its precise potential control, PFE has been particularly important in characterizing the kinetics and thermodynamics of the inactivation reactions of uptake [NiFe]-hydrogenases. The anaerobic oxidative inactivation of uptake [NiFe]-hydrogenases such as that from *Allochromatium vinosum* to form Ni-B can often be observed in cyclic voltammetry experiments at extremely slow scan rates, i.e., 0.3 mV s^{-1}, as a decrease in the hydrogen oxidation current at high potentials and a concomitant return of activity at lower potentials as the enzyme is reactivated (see, for example, ref 36). However, no such signs of inactivation (or reactivation) were detected in *anaerobic* cyclic voltammetry experiments with HoxEFUYH. We note however, that the experiments in this work were completed at a significantly faster scan rate: 10 mV s^{-1}. Attempts to utilize slower scan rates resulted in significant irreversible film loss prohibiting a meaningful interpretation of the data. Since Ni-B is believed to contain a bridging hydroxide ligand in the active site and hydrogen is thought to provide protection against its formation, chronoamperometry experiments were undertaken at low hydrogen pressures (5%), and high pH (7.5) to observe an anaerobically oxidatively inactivated state. Figure 7 shows that under these conditions on longer time scales (ca. 10−20 min) HoxEFUYH could be anaerobically inactivated at oxidative potentials and reactivated by brief exposure to reducing conditions. First, hydrogen oxidation activity was observed at +147 mV for 900 s. The observed decay of activity with time is thought to be a combination of irreversible "film loss" (either denaturation of enzyme on the electrode surface or diffusion of enzyme away from the electrode surface) and reversible anaerobic inactivation of the active site. Then, the potential was briefly stepped to −563 mV for 180 s to reactivate enzyme. Upon return of the potential to +147 mV, increased catalytic activity corresponding to reactivation of the enzyme film at low potentials was observed (circled area in Figure 7). The range of conditions for formation of this inactive state is relatively narrow. Either an increase of the pressure of hydrogen or decrease of the solution pH prevented formation of this state.

Figure 8 provides evidence that two inactive states of HoxEFUYH are formed in the presence of oxygen. Cyclic voltammetry in 5% H_2 at pH 7.5 was initiated at the reducing limit at a scan rate of 5 mV/s. At a potential of approximately −200 mV, air saturated buffer was injected to a final oxygen concentration of 14 μM. Catalytic activity halted immediately (data not shown). The buffer was then exchanged to an oxygen free solution, and the experiment recommenced from the oxidative limit as shown in Figure 8. Initially, the enzyme was completely inactive, and no catalytic current was observed. However, at approximately −100 mV, nearly 275 mV more oxidizing than the potential for reductive reactivation of the aerobically produced state determined above (Figure 6), a small amount of catalytic activity began to reappear. Then, at much lower potentials, i.e., below even the potential of the hydrogen couple, the bulk of the enzyme was reactivated, and, on the return scan, substantial catalytic activity was observed again. However, just as for the anaerobic chronoamperometry experiments, under less basic conditions (pH 5−7), evidence of inactivation and reactivation was not

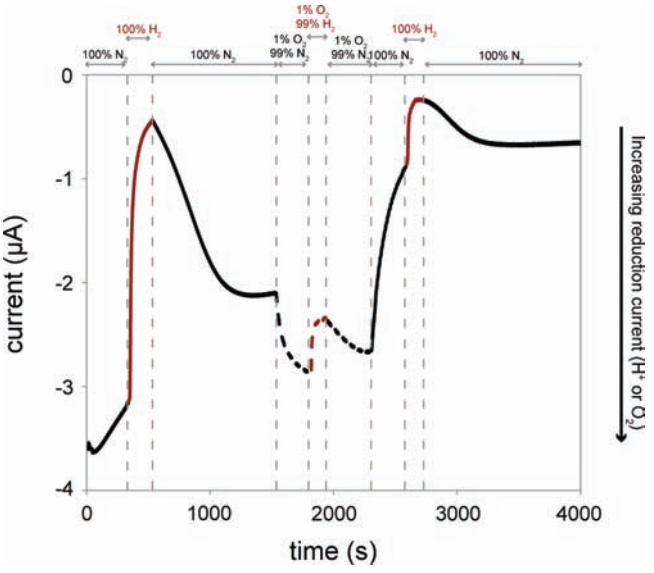

Figure 9. Demonstration of the ability of HoxEFUYH to produce hydrogen in the presence of 1% O_2. Experimental conditions: mixed buffer pH 5.4 at 25 °C; electrode potential, −453 mV vs SHE; electrode rotation rate, 1600 rpm. Nitrogen was first bubbled through the cell (black solid line) followed by H_2 (red solid line) and the swift decrease seen in reduction current is due to H_2 inhibition of H^+ reduction. The H_2 was then removed with a stream of N_2 until a stable current was obtained, after which the gas was switched to 1% O_2 in N_2 (black dashed line). To discern whether the hydrogenase was still functioning under these conditions, the gas stream was then switched to 1% O_2 in H_2 (red dashed line) to inhibit any active enzyme. The gas was then switched back to 1% O_2 in N_2 to demonstrate the reversible inhibition and that the decrease in current was not due to some other process. The 1% O_2 was then bubbled out of the cell with 100% N_2.

apparent in analogous experiments. These results clearly demonstrate that two distinct inactive species are formed with unique reactivation characteristics. The properties of the higher potential reactivating state are the subject of ongoing investigation.

4. H_2 Production by HoxEFUYH in the Presence of O_2. Since HoxEFUYH is believed to play a role in transitioning between light/dark and aerobic/anaerobic metabolisms, the ability of the enzyme to produce hydrogen in the presence of O_2 was investigated. As shown in Figure 9, HoxEFUYH can continuously reduce H^+ in the presence of 1% O_2. In this chronoamperometry experiment, the enzyme was held at a constant, reducing potential (−453 mV) throughout, and the gas atmosphere above the cell was changed. In the first part of the investigation, the enzyme was kept under a N_2 atmosphere and the negative reduction current displayed is exclusively due to the enzyme reducing H^+ to H_2. To inhibit the enzyme, the gas stream was switched to H_2 (red in the figure) and the swift loss in negative current is the result of H_2 inhibition of HoxEFUYH, as shown also above (see also Figure 4). It is important to note here that even under 1 atm of H_2 at the pH used in the experiment, the H^+ reduction activity of HoxEFUYH was not fully inhibited, as indicated by residual negative current. After inhibiting the enzyme, the gas stream was switched back to N_2 and the H_2 was slowly bubbled away. Once a steady reduction current was obtained, indicating complete removal of the inhibitor, the gas stream was again changed, this time to 1% O_2 in N_2 (black dashed line in the figure). The increase in reduction current is due to direct reduction of O_2 on the PGE electrode. To determine the amount of reductive current attributable to the enzyme under these conditions, the gas stream was switched to 1% O_2 in H_2 (inhibiting the enzyme) and the current monitored. As illustrated by the red dashed line in the Figure 9, the approximately 0.5 μA of current lost in this step is due to inhibition of HoxEFUYH functioning under 1% O_2. The 1% O_2 in H_2 was then replaced with 1% O_2 in N_2 and, once stable current was obtained, the O_2 was removed by switching the gas atmosphere back to 100% N_2. After removing the O_2, the gas stream was again exchanged, first to H_2 to inhibit and then to N_2 to demonstrate the amount of active enzyme after O_2 removal (the final red and black solid lines). Assuming that 99% H_2 fully inhibits the enzyme (which it does not), 25−50% of the enzyme functions in the presence of 1% O_2 (limits determined based on the current due to enzyme activity before the introduction of O_2 and on the current obtained before the final inhibition step, respectively), which compares well with the estimates obtained by Parkin and co-workers in a similar experiment for a [NiFeSe]-hydrogenase (17 and 42%, respectively).[38]

DISCUSSION

Although bidirectional [NiFe]-hydrogenases are biologically widespread, intimately involved in photobiological production of hydrogen and potentially of relevance to solar biotechnological applications, our results represent the first electrochemical characterization of either a member of this group or a [NiFe]-hydrogenase from an aerobic phototroph. The electrochemical investigation of HoxEFUYH from *Synechocystis* sp. PCC 6803 has revealed important, and perhaps unexpected, properties, each of which will be considered in turn below.

The first unexpected property of HoxEFUYH catalysis is that the hydrogen production rate at low pH and negligible hydrogen pressure (ideal conditions for reductive catalysis) is approximately 1.4 times faster than the hydrogen oxidation rate at high pH and hydrogen pressure (ideal conditions for oxidative catalysis). Thus HoxEFUYH is the first [NiFe]-hydrogenase studied that can be characterized as a hydrogen-producing enzyme. However, this bias toward production is so moderate that it may be more accurate to think of HoxEFUYH as a truly bidirectional enzyme much like *Escherichia coli* Hyd-2.[30] Although the mechanism for controlling bias in [NiFe]-hydrogenases remains unclear, from a physiological perspective, the reductive bias of HoxEFUYH should perhaps not be surprising since it has been proposed to serve as an electron valve for excess reducing equivalents. Alternatively, a possible role in interfacing with Complex I in the membrane may also require the unusual catalytic bias of this enzyme.[45,46,51]

The reactions of HoxEFUYH with oxygen are also different from what might have been expected based on either FTIR data[57,62] or comparison to either "standard uptake " or "oxygen-tolerant" enzymes (see Scheme 1 for a summary of the spectroscopically observed states from the various types of hydrogenases). Standard uptake [NiFe]-hydrogenases form two distinct, EPR-active, inactive states. Ni-A, also referred to as "unready", reactivates slowly under reducing conditions whereas Ni-B, also referred to as the "ready" state, is quickly reactivated. On the other hand, "oxygen-tolerant" [NiFe]-hydrogenases such as that from *Aquifex aeolicus* are aerobically inactivated to a single state, Ni-B, that is thought to be identical to the state formed during anaerobic inactivation.[32] Both Ni-B and Ni-A are characterized by EPR signals arising from Ni(III). Ni-B is believed to contain a (hydr)oxo bridging ligand in the active site, and Ni-A, although a matter of ongoing debate, a (hydro)peroxo bridging

species.[72,73] Preliminary FTIR investigations of HoxEFUYH and the highly homologous soluble hydrogenase from *Ralstonia eutropha* (*Re*SH) have suggested that these enzymes, like oxygen-tolerant ones, can only be oxidized to a single state referred to as "Ni-B-like".[62] However, the Ni-B-like state is distinguished from the standard Ni-B state in that it does not have an accompanying EPR signal, and the positions of the IR bands are slightly shifted, a result attributed to the specific amino acid environment of the active site.[57] Additionally, unlike the "oxygen-tolerant" enzymes, both HoxEFUYH and *Re*SH require reactivation to observe catalytic activity after aerobic purification. In contrast to the FTIR results, our electrochemical results show that *two distinct* states are formed upon reaction of HoxEFUYH with oxygen, but these two states have different properties than the classical Ni-A and Ni-B. First, both states are quickly reactivated. Second, the states are reactivated at two distinct reduction potentials. The minor species is reactivated at high potentials much like a classical Ni-B, and the predominant species is reactivated at potentials below even the hydrogen couple. In thermodynamic terms, this is the reason that HoxEFUYH, unlike the oxygen-tolerant enzymes, cannot oxidize hydrogen in the presence of oxygen. The observation that HoxEFUYH can be quickly reactivated after aerobic inactivation is different from standard uptake hydrogenases and may be a feature of physiological relevance for cyanobacteria. Gutthann and co-workers demonstrated that upon one minute of anaerobic dark incubation hydrogen production can be observed in the cyanobacterium *Synechocystis*.[49] Similarly, measurements of oxygen concentrations have been made with cyanobacterial mats, which are important microbial communities. It has been demonstrated that upon a transition to the dark, oxygen concentrations in the top, oxic zone of mats can drop from more than 600 μM to anoxic in a matter of three to four minutes.[74] A standard [NiFe]-hydrogenase requiring tens of minutes to be reactivated from the N-A state might be too slow to react to these changing redox potentials inside the cell. However, HoxEFUYH is perfectly positioned to do so. The enzyme is firmly in the inactive, off state under aerobic photosynthetic conditions, but can rapidly be turned on again as soon as the cell establishes an anaerobic, or even microaerobic, environment. Since transitions between aerobic and anaerobic conditions in natural aquatic environmental ecosystems may be expected to occur regularly as light intensity fluctuates, a cyanobacterial hydrogenase must then be poised to function quickly under changing physiological conditions and that corresponds with the biochemical properties we have observed.

The electrochemical results beg the question why only one aerobically inactivated state for HoxEFUYH was detected in the FTIR experiments.[57] The answer may lie in the relative proportions of the two species and the difficulty in forming the higher potential reactivating state. First, the higher potential reactivating state was only observed under alkaline conditions with very low pressures of hydrogen. These are conditions that may not have been generated in the FTIR experiments, in which inactivation occurred because oxygen was allowed to slowly leak into the cell. Second, the relatively small amount of catalytic activity recovered by reactivation of the high potential reactivating species (Figure 7) suggests that this species probably accounts for less than 5% of the inactivated enzyme. Thus within the sensitivity of the FTIR experiment and the potential control of the spectroscopic apparatus, we should probably not expect the higher potential reactivating species to be observed to any significant extent. A third explanation for the observation of two inactive states is that the high potential reactivating state does not form in solution experiments because it is an artifact of adsorption of the enzyme onto the electrode surface. In support of this hypothesis, Lauterbach and co-workers have recently characterized the hydrogenase dimer subcomplex (HoxHY) of the soluble bidirectional hydrogenase (SH) from *Ralstonia eutropha*.[55] Although FTIR investigations of the complete heterohexameric SH detected only a single inactive state, experiments with the HoxHY subcomplex identified two inactive species. Thus it is possible that formation of the second inactive form is only possible for degraded enzymes in which the quaternary structure has been altered or the diaphorase unit inactivated. This might suggest that on the electrode surface, the quaternary structure of HoxEFUYH is changed relative to the structure found in solution. Exploration of this hypothesis is ongoing in our laboratory. With this in mind, it is also important to consider which of the two inactive species observed electrochemically was observed in the FTIR experiments. Although the spectroscopically observed state has been termed "Ni-B-like", the evidence suggests that this spectroscopic state corresponds to the lower potential reactivating state observed in the electrochemical experiments: an exclusively aerobically formed state perhaps more akin to Ni-A. The analogy to the Ni-B state of standard uptake hydrogenases is primarily in the similarity of the FTIR frequencies of the diatomic ligands and the speed with which the state is reactivated. However, the electrochemical results indicate that the lower potential reactivating state of HoxEFUYH, unlike classical Ni-A, is also very quickly reactivated. It is clear the inactive states of HoxEFUYH are different from those of other hydrogenases characterized to date, and we will return to hypotheses for this difference shortly.

Despite the fact that HoxEFUYH is not what has traditionally been called an "oxygen-tolerant" enzyme, it is able to reduce protons in the presence of 1% oxygen at rates 25−50% of those in the absence of the inhibitor. Only three other hydrogenases have been conclusively demonstrated to perform reductive catalysis in the presence of oxygen: the membrane bound hydrogenase from *Ralstonia eutropha* (*Re*MBH), a stereotypical uptake, oxygen-tolerant enzyme,[26] the [NiFeSe]-hydrogenase from *Desulfomicrobium baculatum*,[38] and Hyd-2 from *Escherichia coli*,[30] all three heterodimeric, uptake enzymes. When considering the electrochemical properties of HoxEFUYH generally, a series of striking similarities to the [NiFeSe]-hydrogenases from *Desulfomicrobium baculatum* and *Desulfovibrio vulgaris* arises. Like HoxEFUYH, both [NiFeSe]-enzymes have been the subject of recent investigations structurally, spectroscopically, and electrochemically and have been demonstrated to efficiently catalyze proton reduction even in the presence of oxygen.[38,75,76] For *Desulfomicrobium baculatum* [NiFeSe]-hydrogenase, Parkin and co-workers have argued that the efficient proton reduction catalysis and the ability to maintain this catalysis in the presence of oxygen, properties shared with HoxEFUYH but not with the other standard uptake hydrogenases, are both consequences of the unique, terminally nickel ligating selenocysteine. They hypothesize that the substantially lower pK_a of selenocysteine relative to the cysteine in the standard uptake enzymes is the main contributing factor in the unique properties of [NiFeSe]-hydrogenases.[38] The [NiFeSe]-hydrogenase from *Desulfomicrobium baculatum* also shares an extremely similar O_2 inactivation profile with HoxEFUYH, forming two inactive oxidized states that are quickly reactivated at two separate reduction potentials. In the recently reported crystal structure of the aerobically as-

isolated version of the [NiFeSe]-hydrogenase from *Desulfovibrio vulgaris*, the authors assign both these oxidized states to active sites with oxidized terminal Ni ligands, and a bridging O_2/H_2O derived ligand such as described for standard uptake [NiFe]-hydrogenases was not observed.[76] In the major conformer determined from the structural investigation (70% occupation), a five-coordiate Ni was bound with an extra S ligand and the terminal Cys75 was persulfurated. The authors posit that binding of the extra S ligand leads to movement of the Se to a position that prevents attack on the [NiFe] bridging position by small molecule inhibitors (and the larger atomic radius of Se compared with S may also play a role). Needless to say, HoxEFUYH *does not* contain a Se within its active site. However, even for the standard uptake [NiFe] enzymes there continues to be much debate as to the nature of the oxidized, inactive forms, especially the slowly reactivating Ni-A. Ogata and co-workers have recently reported that the crystal structure of the uptake [NiFe]-hydrogenase from the anaerobic photosynthetic bacterium *Allochromatium vinosum* in the Ni-A state contains a mono-oxo bridging ligand in contrast to the peroxo ligand reported for the enzymes from *Desulfovibrio* sp.[73] Additionally, partial oxidative modification of a Ni-coordinating cysteine was observed, and alternative conformations for the proximal [4Fe4S] clusters were also detected. This may suggest irreversible damage to the crystals occurred during X-ray exposure, but these results serve nonetheless to highlight the possibility that a range of different, perhaps even physiologically relevant, oxidative modifications may occur in [NiFe]-hydrogenases. The chemical states that a particular enzyme is able to form may be linked to both its unique biological role and its structural features. Unfortunately, no structural information has been reported for an oxygen-tolerant uptake enzyme, a bidirectional enzyme, or an enzyme from an aerobic phototroph. It would be wild speculation to comment on the chemical features of the inactive states of HoxEFUYH, but it is possible that such chemical differences at the active site are the cause of the unusual reactivation kinetics observed for HoxEFUYH.

FTIR spectroscopic investigations of [NiFe]-hydrogenases have shown that all enzymes studied to date, including the standard uptake, the oxygen-tolerant uptake enzymes, and the bidirectional HoxEFUYH, despite differing reactivities, share a largely conserved active site architecture. Thus it may also be possible that the unusual reactivity of HoxEFUYH is a property not of the active site but of the additional [FeS] cluster coordinating subunits. Recent studies of the oxygen-tolerant hydrogenases have suggested that their unique reactivity may be attributed to a relatively conserved pair of cysteines located near the proximal [4Fe4S] cluster.[77−79] Additionally, Liebgott and co-workers have demonstrated that mutation of a single residue located roughly between the [NiFe] site and the proximal [4Fe4S] cluster in the active site containing subunit created variant proteins that were intermediate in their reactivity toward oxygen. The authors hypothesize that, in oxygen-tolerant [NiFe]-hydrogenases, amino acids near the electron transfer conduit may specifically tune the rate of electron transfer through the iron sulfur clusters to allow complete reduction of oxygen once it enters the active site, thus facilitating faster reactivation. This modulation of electron transfer could be achieved via modification of the reduction potential of the nearby [4Fe4S] cluster, variation of the electronic coupling between redox centers or a change in the reorganization energy.[33,78] Such a hypothesis is also appealing to explain the unique properties of HoxEFUYH. Although the standard, uptake [NiFe]-hydrogenases usually contain two [4Fe4S] clusters and a higher potential [3Fe4S] cluster, HoxEFUYH is believed to contain only [4Fe4S] and [2Fe2S] clusters, many of which have escaped detection by EPR. An as yet uncharacterized coupling between one of the [FeS] clusters and the [NiFe] site could explain the lack of observable Ni(III) EPR signals and might also have a dramatic impact on intramolecular electron transfer. Alternatively, the unique complement of [FeS] clusters in HoxEFUYH, especially the absence of a [3Fe4S] cluster, may effect intramolecular electron transfer to the active site such that a stable Ni(III) state is indeed never formed. In support of these hypotheses, Dementin and co-workers have demonstrated that merely changing the coordination of the terminal [4Fe4S] cluster from a histidine to a cysteine, dramatically affects the intramolecular electron transfer rate for the *Desulfovibrio fructosovorans* [NiFe]-hydrogenase.[80] Additionally, Rousset and co-workers converted the medial [3Fe4S] cluster of the same enzyme to a [4Fe4S] cluster and saw a slight shift in the catalytic bias of the enzyme away from hydrogen oxidation to proton reduction.[81] Finally, the [NiFeSe]-hydrogenases characterized to date, like HoxEFUYH, are also devoid of [3Fe4S] clusters and Ni(III) EPR signals. This is a remarkable coincidence in light of their undeniable catalytic similarities and suggests that the catalytic bias toward proton reduction and the inability to form a slowly reactivating state observed for both of these types of enzymes may have a common mechanism related to the lack of a [3Fe4S] cluster.

Although HoxEFUYH is the only multimeric bidirectional [NiFe]-hydrogenase that has been electrochemically characterized to date, as mentioned above, the closely related hydrogenase subcomplex, HoxHY, of the heterohexameric, soluble, bidirectional [NiFe]-hydrogenase (SH) from *Ralstonia eutropha* has also been recently investigated via electrochemistry and FTIR spectroscopy.[55] Interestingly, there are several similarities to the *Synechocystis* HoxEFUYH. First, both enzymes are efficient in the hydrogen production direction. Second, both enzymes maintain significant proton reduction activity even in an atmosphere of 100% hydrogen. Third, both enzymes appear to form two oxidatively inactivated states under aerobic conditions that are very rapidly reactivated under reducing conditions. It is tempting to conclude that these may be defining features of the bidirectional, multimeric enzymes. However, the observation that the two most oxidized states of *Ralstonia eutropha* HoxHY observed via FTIR are not observed in samples of the intact hexameric enzyme either *in vivo* or *in vitro* is sufficient reason to question any such conclusion. If the accessory Fe−S domains are indeed relevant in modulating reactivity at the [NiFe] site, then deletion of these domains may have unknown and unexpected impacts on enzyme stability and function. With this in mind, we are cautious to generalize our conclusions and look forward to seeing more detailed investigations of other bidirectional [NiFe]-hydrogenases.

In conclusion, we have presented the catalytic properties of the bidirectional HoxEFUYH from *Synechocystis* sp. PCC 6803. Although the enzyme shares a [NiFe] active site coordination with its "standard" uptake hydrogenase relatives, its catalytic bias and inactive oxidized states are significantly different from that of its cousins. The potential technological applications of organisms capable of producing H_2 from solar energy in aerobic environments, such as cyanobacteria, make establishing the mechanistic underpinnings of these differences essential. The answers may not easily be found in the structures and environments of the redox cofactors themselves but in the interactions between the many redox cofactors in HoxEFUYH that facilitate fast proton

and electron transfer. In light of recent suggestions that oxygen tolerance in some [NiFe]-hydrogenases, for example, is a property not of the active site or of gas tunnels leading to the active site but of the protein environment surrounding the proximal [FeS] cluster, closer attention must be paid to characterizing the interactions between the [FeS] clusters and the [NiFe] site in HoxEFUYH. It is also interesting to postulate whether the traits of the enzyme put forth in this investigtion are unique to HoxEFUYH, having evolved to fit the role it plays *in vivo* in an aerobic phototroph, or if, in fact, this phenotype is characteristic of all the group 3 multimeric bidirectional hydrogenases and perhaps related to their linkage to the diaphorase functional unit. Given the similar lack of Ni(III) EPR data for all bidirectional hydrogenases studied so far, one might easily assume that most bidirectional enzymes will follow this paradigm, though conclusive evidence will have to come from the characterization of others.

■ ASSOCIATED CONTENT

Supporting Information. Chronoamperometry control experiments, table of extrapolated absolute currents for catalytic experiments, and complete ref 28. This material is available free of charge via the Internet at http://pubs.acs.org.

■ AUTHOR INFORMATION

Corresponding Author
jonesak@asu.edu

■ ACKNOWLEDGMENT

C.L.M. thanks the Science Foundation of Arizona for a graduate fellowship. C.L.M. and A.K.J. were supported in part through the Center for Bio-Inspired Solar Fuel Production, an Energy Frontier Research Center funded by the U.S. Department of Energy, Office of Science, Office of Basic Energy Sciences, under Award No. DE-SC0001016. The work of F.G. was financially supported by Linde AG and by the foundation of the Universität Kiel and the German state of Schleswig-Holstein. J.A. acknowledges the generous support of the Brian and Kelly Swette foundation.

■ REFERENCES

(1) Fontecilla-Camps, J. C.; Volbeda, A.; Cavazza, C.; Nicolet, Y. *Chem. Rev.* **2007**, *107*, 4273–4303.
(2) Jones, A. K.; Sillery, E.; Albracht, S. P. J.; Armstrong, F. A. *Chem. Commun.* **2002**, 866–867.
(3) Vincent, K. A.; Parkin, A.; Armstrong, F. A. *Chem. Rev.* **2007**, *107*, 4366–4413.
(4) Hambourger, M.; Gervaldo, M.; Svedruzic, D.; King, P. W.; Gust, D.; Ghirardi, M.; Moore, A. L.; Moore, T. A. *J. Am. Chem. Soc.* **2008**, *130*, 2015–2022.
(5) Reisner, E.; Powell, D. J.; Cavazza, C.; Fontecilla-Camps, J. C.; Armstrong, F. A. *J. Am. Chem. Soc.* **2009**, *131*, 18457–18466.
(6) Wait, A. F.; Parkin, A.; Morley, G. M.; dos Santos, L.; Armstrong, F. A. *J. Phys. Chem. C* **2010**, *114*, 12003–12009.
(7) Ihara, M.; Nishihara, H.; Yoon, K. S.; Lenz, O.; Friedrich, B.; Nakamoto, H.; Kojima, K.; Honma, D.; Kamachi, T.; Okura, I. *Photochem. Photobiol.* **2006**, *82*, 676–682.
(8) Krassen, H.; Schwarze, A.; Friedrich, B.; Ataka, K.; Lenz, O.; Heberle, J. *ACS Nano* **2009**, *3*, 4055–4061.
(9) Gust, D.; Moore, T. A.; Moore, A. L. *Acc. Chem. Res.* **2009**, *42*, 1890–1898.
(10) Lubner, C. E.; Grimme, R.; Bryant, D. A.; Golbeck, J. H. *Biochemistry* **2010**, *49*, 404–414.
(11) Lee, H.-S.; Vermaas, W. F. J.; Rittmann, B. E. *Trends Biotechnol.* **2010**, *28*, 262–271.
(12) Houchins, J. P. *Biochim. Biophys. Acta* **1984**, *768*, 227–255.
(13) Happe, T.; Naber, J. D. *Eur. J. Biochem.* **1993**, *214*, 475–481.
(14) Schutz, K.; Happe, T.; Troshina, O.; Lindblad, P.; Leitao, E.; Oliveira, P.; Tamagnini, P. *Planta* **2004**, *218*, 350–359.
(15) Ghirardi, M.; Posewitz, M. C.; Maness, P.-C.; Dubini, A.; Yu, J.; Seibert, M. *Annu. Rev. Plant Biol.* **2007**, *58*, 71–91.
(16) Hemschemeier, A.; Melis, A.; Happe, T. *Photosynth. Res.* **2009**, *102*, 523–540.
(17) Melis, A. *Planta* **2007**, *226*, 1075–1086.
(18) Vincent, K. A.; Parkin, A.; Lenz, O.; Albracht, S. P. J.; Fontecilla-Camps, J. C.; Cammack, R.; Friedrich, B.; Armstrong, F. A. *J. Am. Chem. Soc.* **2005**, *127*, 18179–18189.
(19) Parkin, A.; Cavazza, C.; Fontecilla-Camps, J. C.; Armstrong, F. A. *J. Am. Chem. Soc.* **2006**, *128*, 16808–16815.
(20) Goldet, G.; Brandmayr, C.; Stripp, S. T.; Happe, T.; Cavazza, C.; Fontecilla-Camps, J. C.; Armstrong, F. A. *J. Am. Chem. Soc.* **2009**, *131*, 14979–14989.
(21) Silakov, A.; Kamp, C.; Reijerse, E.; Happe, T.; Lubitz, W. *Biochemistry* **2009**, *48*, 7780–7786.
(22) Stripp, S. T.; Goldet, G.; Brandmayr, C.; Sanganas, O.; Vincent, K. A.; Haumann, M.; Armstrong, F. A.; Happe, T. *Proc. Natl. Acad. Sci. U.S.A.* **2009**, *106*, 17331–17336.
(23) Shepard, E. M.; McGlynn, S. E.; Bueling, A. L.; Grady-Smith, C. S.; George, S. J.; Winslow, M. A.; Cramer, S. P.; Peters, J. W.; Broderick, J. B. *Proc. Natl. Acad. Sci. U.S.A.* **2010**, *107*, 10448–10453.
(24) Mulder, D. W.; Boyd, E. S.; Sarma, R.; Lange, R. K.; Endrizzi, J. A.; Broderick, J. B.; Peters, J. W. *Nature* **2010**, *465*, 248–252.
(25) Burgdorf, T.; Loescher, S.; Liebisch, P.; van der Linden, E.; Galander, M.; Lendzian, F.; Meyer-Klaucke, W.; Albracht, S. P. J.; Friedrich, B.; Dau, H.; Haumann, M. *J. Am. Chem. Soc.* **2005**, *127*, 576–592.
(26) Goldet, G.; Wait, A. F.; Cracknell, J. A.; Vincent, K. A.; Ludwig, M.; Lenz, O.; Friedrich, B.; Armstrong, F. A. *J. Am. Chem. Soc.* **2008**, *130*, 11106–11113.
(27) Cracknell, J. A.; Wait, A. F.; Lenz, O.; Friedrich, B.; Armstrong, F. A. *Proc. Natl. Acad. Sci. U.S.A.* **2009**, *106*, 20681–20686.
(28) Dementin, S.; et al. *J. Am. Chem. Soc.* **2009**, *131*, 10156–10164.
(29) Ludwig, M.; Cracknell, J. A.; Vincent, K. A.; Armstrong, F. A.; Lenz, O. *J. Biol. Chem.* **2009**, *284*, 465–477.
(30) Lukey, M. J.; Parkin, A.; Roessler, M. M.; Murphy, B. J.; Harmer, J.; Palmer, T.; Sargent, F.; Armstrong, F. A. *J. Biol. Chem.* **2010**, *285*, 3928–3938.
(31) Fourmond, V.; Infossi, P.; Giudici-Orticoni, M.; Bertrand, P.; Léger, C. *J. Am. Chem. Soc.* **2010**, *132*, 4848–4857.
(32) Pandelia, M.; Fourmond, V.; Tron-Infossi, P.; Lojou, E.; Bertrand, P.; Léger, C.; Giudici-Orticoni, M.; Lubitz, W. *J. Am. Chem. Soc.* **2010**, *132*, 6991–7004.
(33) Liebgott, P.-P.; de Lacey, A. L.; Burlat, B.; Cournac, L.; Richaud, P.; Brugna, M.; Fernandez, V. M.; Guigliarelli, B.; Rousset, M.; Léger, C.; Dementin, S. *J. Am. Chem. Soc.* **2011**, *133*, 986–997.
(34) Pershad, H. R.; Duff, J. L. C.; Heering, H. A.; Duin, E. C.; Albracht, S. P. J.; Armstrong, F. A. *Biochemistry* **1999**, *38*, 8992–8999.
(35) Léger, C.; Jones, A. K.; Roseboom, W.; Albracht, S. P. J.; Armstrong, F. A. *Biochemistry* **2002**, *41*, 15736–15746.
(36) Jones, A. K.; Lamle, S. E.; Pershad, H. R.; Vincent, K. A.; Albracht, S. P. J.; Armstrong, F. A. *J. Am. Chem. Soc.* **2003**, *125*, 8505–8514.
(37) Lamle, S. E.; Albracht, S. P. J.; Armstrong, F. A. *J. Am. Chem. Soc.* **2004**, *126*, 14899–14909.
(38) Parkin, A.; Goldet, G.; Cavazza, C.; Fontecilla-Camps; Armstrong, F. A. *J. Am. Chem. Soc.* **2008**, *130*, 13410–13416.
(39) Léger, C.; Dementin, S.; Bertrand, P.; Rousset, M.; Guigliarelli, B. *J. Am. Chem. Soc.* **2004**, *126*, 12162–12172.
(40) Lenz, O.; Ludwig, M.; Schubert, T.; Burstel, I.; Ganskow, S.; Goris, T.; Schwarze, A.; Friedrich, B. *Chemphyschem* **2010**, *11*, 1107–1119.

(41) Vignais, P.; Billoud, B. *Chem. Rev.* **2007**, *107*, 4206–4272.
(42) Appel, J. The physiology and functional genomics of cyanobacterial hydrogenases and approaches towards biohydrgoen production. In *Functional Genomics and Evolution of Photosynthetic Systems*; Burnap, R. L., Vermaas, W. F. J., Eds.; Advances in Photosynthesis and Respiration 33; Springer: Berlin, 2011.
(43) Ludwig, M.; Schulz-Friedrich, R.; Appel, J. *J. Mol. Evol.* **2006**, *63*, 758–768.
(44) Barz, M.; Beimgraben, C.; Staller, T.; Germer, F.; Opitz, F.; Marquardt, C.; Schwarz, C.; Gutekunst, K.; Vanselow, K. H.; Schmitz, R.; Laroche, J.; Schulz, R.; Appel, J. *PLoS One* **2011**, *5*, e13846.
(45) Appel, J.; Schulz, R. *J. Photochem. Photobiol. B* **1998**, *47*, 1–11.
(46) Appel, J.; Phunpruch, S.; Steinmuller, K.; Schulz, R. *Arch. Microbiol.* **2000**, *173*, 333–338.
(47) Cournac, L.; Mus, F.; Bernard, L.; Guedeney, G.; Vignais, P.; Peltier, G. *Int. J. Hydrogen Energ* **2002**, *27*, 1229–1237.
(48) Cournac, L.; Guedeney, G.; Peltier, G.; Vignais, P. *J. Bacteriol.* **2004**, *186*, 1737–1746.
(49) Gutthann, F.; Egert, M.; Marques, A.; Appel, J. *Biochim. Biophys. Acta* **2007**, *1767*, 161–169.
(50) Schmitz, O.; Boison, G.; Hilscher, R.; Hundeshagen, B.; Zimmer, W.; Lottspeich, F.; Bothe, H. *Eur. J. Biochem.* **1995**, *233*, 266–276.
(51) Appel, J.; Schulz, R. *Biochim. Biophys. Acta* **1996**, *1298*, 141–147.
(52) Schmitz, O.; Boison, G.; Salzmann, H.; Bothe, H.; Schuetz, K.; Wang, S.-H.; Happe, T. *Biochim. Biophys. Acta* **2002**, *1554*, 66–74.
(53) Löscher, S.; Burgdorf, T.; Zebger, I.; Hildebrandt, P.; Dau, H.; Friedrich, B.; Haumann, M. *Biochemistry* **2006**, *45*, 11658–11665.
(54) van der Linden, E.; Burgdorf, T.; de Lacey, A. L.; Buhrke, T.; Scholte, M.; Fernandez, V. M.; Friedrich, B.; Albracht, S. P. J. *J. Biol. Inorg. Chem.* **2006**, *11*, 247–260.
(55) Lauterbach, L.; Liu, J.; Horch, M.; Hummel, P.; Schwarze, A.; Haumann, M.; Vincent, K. A.; Lenz, O.; Zebger, I. *Eur. J. Inorg. Chem.* **2011**, *7*, 1067–1079.
(56) Vignais, P.; Colbeau, A. *Curr. Issues Mol. Biol.* **2004**, *6*, 159–188.
(57) Germer, F.; Zebger, I.; Saggu, M.; Lendzian, F.; Schulz, R.; Appel, J. *J. Biol. Chem.* **2009**, *284*, 36462–36472.
(58) Serebryakova, L. T.; Medina, M.; Zorin, N. A.; Gogotov, I. N.; Cammack, R. *FEBS Lett.* **1996**, *383*, 79–82.
(59) Bryant, F. O.; Adams, M. W. W. *J. Biol. Chem.* **1989**, *264*, 5070–5079.
(60) Schneider, K.; Cammack, R.; Schlegel, H. G. *Eur. J. Biochem.* **1984**, *142*, 75–84.
(61) Long, M.; Liu, J.; Chen, Z.; Bleijlevens, B.; Roseboom, W.; Albracht, S. P. J. *J. Biol. Inorg. Chem.* **2007**, *12*, 62–78.
(62) Horch, M.; Lauterbach, L.; Saggu, M.; Hildebrandt, P.; Lendzian, F.; Bittl, R.; Lenz, O.; Zebger, I. *Angew. Chem., Int. Ed.* **2010**, *49*, 8026–8029.
(63) Page, C. C.; Moser, C. C.; Chen, X.; Dutton, P. L. *Nature* **1999**, *402*, 47–52.
(64) Léger, C.; Elliott, S. J.; Hoke, K. R.; Jeuken, L. J. C.; Jones, A. K.; Armstrong, F. A. *Biochemistry* **2003**, *42*, 8653–8662.
(65) Léger, C.; Bertrand, P. *Chem. Rev.* **2008**, *108*, 2379–2438.
(66) Armstrong, F. A.; Belsey, N. A.; Cracknell, J. A.; Goldet, G.; Parkin, A.; Reisner, E.; Vincent, K. A.; Wait, A. F. *Chem. Soc. Rev.* **2009**, *38*, 36–51.
(67) Bard, A. J.; Faulkner, L. R., *Electrochemical methods. Fundamentals and applications*; John Wiley & Sons, Inc.: New York, 2001.
(68) Fourmond, V.; Hoke, K. R.; Heering, H. A.; Baffert, C.; Leroux, F.; Bertrand, P.; Léger, C. *Bioelectrochemistry* **2009**, *76*, 141–147.
(69) Armstrong, F. A.; Heering, H. A.; Hirst, J. *Chem. Soc. Rev.* **1997**, *26*, 169–179.
(70) Léger, C.; Jones, A. K.; Albracht, S. P. J.; Armstrong, F. A. *J. Phys. Chem. B* **2002**, *106*, 13058–13063.
(71) De Lacey, A. L.; Fernandez, V. M.; Rousset, M.; Cammack, R. *Chem. Rev.* **2007**, *107*, 4304–4330.
(72) Volbeda, A.; Martin, L.; Cavazza, C.; Matho, M.; Faber, B. W.; Roseboom, W.; Albracht, S. P. J.; Garcin, E.; Rousset, M.; Fontecilla-Camps, J. C. *J. Biol. Inorg. Chem.* **2005**, *10*, 239–249.
(73) Ogata, H.; Kellers, P.; Lubitz, W. *J. Mol. Biol.* **2010**, *402*, 428–444.
(74) Epping, E. H. G.; Khalili, A.; Thar, R. *Limnol. Oceanogr.* **1999**, *44*, 1936–1948.
(75) Gutierrez-Sanchez, C.; Rudiger, O.; Fernandez, V. M.; de Lacey, A. L.; Marques, M. C.; Pereira, I. A. C. *J. Biol. Inorg. Chem.* **2010**, *15*, 1285–1292.
(76) Marques, M. C.; Coelho, R.; de Lacey, A. L.; Pereira, I. A. C.; Matias, P. M. *J. Mol. Biol.* **2010**, *396*, 893–907.
(77) Saggu, M.; Zebger, I.; Ludwig, M.; Lenz, O.; Friedrich, B.; Hildebrandt, P.; Lendzian, F. *J. Biol. Chem.* **2009**, *284*, 16264–16276.
(78) Pandelia, M. E.; Nitschke, W.; Infossi, P.; Giudici-Orticoni, M. T.; Bill, E.; Lubitz, W. *Proc. Natl. Acad. Sci. U.S.A.* **2011**, *108*, 6097–6102.
(79) Goris, T.; Wait, A. F.; Saggu, M.; Fritsch, J.; Heidary, N.; Stein, M.; Zebger, I.; Lendzian, F.; Armstrong, F. A.; Friedrich, B.; Lenz, O. *Nat. Chem. Biol.* **2011**, *7*, 310–U87.
(80) Dementin, S.; Belle, V.; Bertrand, P.; Guigliarelli, B.; Adryanczyk-Perrier, G.; De Lacey, A. L.; Fernandez, V. M.; Rousset, M.; Léger, C. *J. Am. Chem. Soc.* **2006**, *128* (15), 5209–5218.
(81) Rousset, M.; Montet, Y.; Guigliarelli, B.; Forget, N.; Asso, M.; Bertrand, P.; Fontecilla-Camps, J. C.; Hatchikian, E. C. *Proc. Natl. Acad. Sci. U.S.A.* **1998**, *95*, 11625–11630.